SIAM J. APPL. MATH.
Vol. 83, No. 6, pp. 2212–2236

GLOBAL DYNAMICS AND PATTERN FORMATION IN A DIFFUSIVE POPULATION-TOXICANT MODEL WITH NEGATIVE TOXICANT-TAXIS*

XIUMEI DENG†, QIHUA HUANG‡, AND ZHI-AN WANG§

Abstract. Because of the significance of remediating contaminated ecosystems, many mathematical models have been developed to describe the interactions between populations and toxicants in polluted aquatic environments. These models typically neglect the consequences of toxicant-induced behavioral changes on population dynamics. Taking into account that individuals may flee from areas with high toxicant concentrations to areas with low toxicant concentrations in order to improve their chances of survival, growth, and reproduction, we develop a diffusive population-toxicant model with toxicant-taxis. We establish the global well-posedness of our model and prove the global stability of spatially homogeneous toxicant-only steady states and population-toxicant coexistence steady states under some conditions. We find conditions under which stable spatially inhomogeneous steady states become unstable to trigger spatial pattern formations as the toxicant-taxis is strong. We also identify a narrow parameter regime in which toxicant-only and population-toxicant coexistence steady states are bistable. Numerical simulations are performed to illustrate that spatial aggregation and segregation patterns between the population and the toxicant will typically emerge. Our study highlights the important effects of toxicant-induced movement responses on the spatial distributions of populations in polluted aquatic environments.

Key words. population-toxicant model, toxicant-taxis, global dynamics, pattern formation, spatial segregation

MSC codes. 92D25, 35K57, 35K2

DOI. 10.1137/22M1510881

1. Introduction.

Rapid industrial development and a variety of human activities have brought a slew of contaminants (e.g., heavy metals, plastic waste, pesticides, etc.) into aquatic environments in recent decades. The detrimental effects of contaminants on the health of aquatic ecosystems, which a large number of species inhabit, are a major concern worldwide. Many countries have enacted water quality standards and regulatory measures to protect aquatic species and ecosystem biodiversity [10, 12, 13, 18, 34, 39, 40]. Toxicants in polluted aquatic environments endanger all levels of the biological hierarchy, from individuals to populations, communities, and entire ecosystems. Understanding the mechanisms of toxicant effects on aquatic species population dynamics, as well as finding the essential factors that determine population persistence and extinction, is crucial from the standpoints of the environment and conservation.

*Received by the editors July 20, 2022; accepted for publication (in revised form) June 30, 2023; published electronically November 15, 2023.
https://doi.org/10.1137/22M1510881
Funding: The work of the second author is partially supported by the National Natural Science Foundation of China grant 12271445. The work of the third author is partially supported by the Hong Kong RGC GRF grant 15306121 and an internal grant from HK PolyU (code W18M).
†School of Mathematics and Statistics, Southwest University, Chongqing 400715, China (xiumeideng95@163.com).
‡Corresponding author. School of Mathematics and Statistics, Southwest University, Chongqing 400715, China (qihua@swu.edu.cn).
§Department of Applied Mathematics, Hong Kong Polytechnic University, Kowloon, Hong Kong (mawza@polyu.edu.hk).

Much of the previous experimental research on the ecological risks of toxicants was performed on individual organisms (e.g., reproduction, survival, and growth) in controlled laboratory settings over relatively short time periods. The design of environmental management strategies, however, requires an understanding of toxicants' impact on the health of entire exposed natural populations in the long term. Mathematical models play a vital role in translating individual responses to population-level consequences. These models include population models (scalar abundance, life history, individual-based, and metapopulation), ecosystem models (food-web, aquatic, and terrestrial), landscape models, and toxicity-extrapolation models [14, 28, 6, 29]. Bartell et al. [6] and Pastorok et al. [29] made a comprehensive review of the realism, relevance, and applicability of various types of models for assessing toxicant risks. Over the last several decades, some (impulsive) differential equation models [15, 16, 17, 20, 21, 25, 27, 36] have been developed to study the dynamical nature of population-toxicant interactions in a polluted aquatic environment. These models usually consist of ordinary differential equations (ODEs) that describe the rates of change of population biomass, the toxicant concentrations in populations, and toxicant concentrations in environments.

The above-mentioned ODE models that describe how toxicants affect population dynamics generally ignore population and toxicant spatial dispersal, whereas both populations and toxicants can spread spatially due to factors such as active mobility and passive diffusion driven by turbulent water. Furthermore, toxicant-induced behavioral changes (e.g., habitat preference, predator avoidance, body tremors, migration) have been well documented [5, 7, 32]. Individuals, for example, may flee from areas with high toxicant concentrations to areas with low toxicant concentrations in order to improve their chances of survival, growth, and reproduction [38]. In this paper, we develop a spatiotemporal model with toxicant-taxis to describe interactions between a population and a toxicant in a contaminated aquatic habitat. The model is made up of two reaction-diffusion equations, one of which governs the growth and movement of the population under the influence of the toxicant, and the other of which describes the toxicant's input, degradation, and dispersal. The model is then used to investigate the effects of toxicants on population persistence and spatial distribution. As far as we know, this model represents the first effort modeling the impact of toxicant-caused behavioral changes on population dynamics by including a toxin-taxis term.

The rest of the paper is organized as follows. In section 2, we formulate a spatiotemporal model with toxicant-taxis for the interaction dynamics between a population and a toxicant in a contaminated aquatic ecosystem and state main analytical results obtained in this paper for our concerned model including global existence of classical solutions and global stability of spatially homogeneous steady states. We then prove the global existence of classical solutions stated in section 3 and show the detailed proofs for the global stability of spatially homogeneous toxicant-only steady states and population-toxicant coexistence steady states in section 4. In section 5, we perform linear stability analysis to identify the parameter regimes under which the stable spatially homogeneous steady states become unstable, and hence pattern formation can be expected. Furthermore, we numerically demonstrate that the spatial aggregation and segregation patterns will typically arise from our model. Finally, in section 6, we discuss model development, outcomes, limitations, and future research directions.

TABLE 2.1
Meanings and units of variables and parameters in model (2.1).

Symbol	Meaning	Unit
$u(t)$	population density at time t	mass/length
$w(t)$	toxicant concentration at time t	mass/length
d_1	diffusion coefficient of the population	length^2/time
χ	taxis coefficient	length^3/(mass·time)
r	intrinsic growth rate	1/time
m	effect coefficient of toxicant on population growth	length/(mass·time)
a	competition coefficient	length/(mass·time)
d_2	diffusion coefficient of the toxicant	length^2/time
$h(x)$	input rate of the toxicant	mass/(length·time)
g	per unit decay rate of the contaminant	1/time
b	uptake coefficient	length/(mass·time)

2. Model formulation and main results. In this section, we shall first introduce our model describing population-toxicant interaction dynamics with toxicant-taxis and then present the main analytical results obtained.

2.1. The model. We consider an aquatic population that inhabits a polluted environment. We use Ω to represent the population habitat, which is a bounded domain in $\mathbb{R}^2$ with smooth boundary, denoted by $\partial\Omega$. Let $u(x,t)$ be the population density at location x and time t. Let $w(x,t)$ be the toxicant concentration at location x and time t. A mathematical model that describes the interaction between the population and the toxicant in the habitat Ω is given by

$$
\begin{cases}
u_t = d_1\Delta u + \chi\nabla\cdot(u\nabla w) + u(r-mw) - au^2, & x\in\Omega,\ t>0,\\
w_t = d_2\Delta w + h(x) - gw - buw, & x\in\Omega,\ t>0,\\
\dfrac{\partial u}{\partial\nu} = \dfrac{\partial w}{\partial\nu} = 0, & x\in\partial\Omega,\ t>0,\\
u(x,0)=u_0(x)\geq\not\equiv 0, w(x,0)=w_0(x)\geq\not\equiv 0, & x\in\Omega.
\end{cases} \tag{2.1}
$$

The model parameters, d_1,χ,r,m,a,d_2,g,b, are all positive constants. Refer to Table 2.1 for meanings and units (for the one-dimensional domain) of the variables and parameters.

The first equation of (2.1) describes the growth rate of the population under the influence of the toxicant. The term $d_1\Delta u$ denotes the random diffusion of the population with coefficient d_1. The toxicant-taxis term $\chi\nabla\cdot(u\nabla w)$ means that the individuals move from locations with high toxicant concentrations to locations with low toxicant concentrations; the direction of population movement is hence inversely proportional to the negative gradient of toxicant, where χ is the taxis coefficient. The term $r-mw$, a linearly decreasing function with respect to the toxicant concentration w, is a toxicant-dependent intrinsic growth rate, where the parameter m is the effect of the toxicant on population growth. If there is no toxic effect, i.e., $w=0$, then the growth rate is the natural growth rate, r. The term au^2 represents the interspecific competition between individuals, which follows the mass action law, where a is used to describe the effect of competition.

The second equation of (2.1) represents a balance equation for the toxicant concentration in the habitat. The parameter d_2 denotes the diffusion coefficient of the toxicant. The function $h(x)$ is the (inhomogeneous) input rate of exogenous toxicant into the environment. The toxicant uptake rate by the population from the environment, buw, is modeled according to the *law of mass action* and hence is proportional to both the toxicant concentration and the population density, where b is the uptake coefficient. The parameter g denotes the per unit output rate of toxicant due to a variety of factors, such as environmental detoxification, microbial degradation, and so on.

The third line of (2.1) is the Neumann boundary conditions corresponding to the first two equations, where $\partial u/\partial\nu = \nabla u(x)\cdot\nu(x)$ is the out-flux of u, and $\nu(x)$ is the outward unit normal vector of $\partial\Omega$ at x, which implies that no individuals enter or leave the habitat Ω across the boundary. A similar meaning is applied for $\partial w/\partial\nu = 0$. The last line of (2.1) gives the initial distributions of the population and the toxicant.

2.2. Main results. The main analytical results obtained for the problem (2.1) consist of two parts: global existence/boundedness of solutions and global stability of spatially homogeneous steady states (i.e., constant equilibria). The former validates that the proposed model (2.1) is globally well-posed, and the latter characterizes the global dynamics of model (2.1). For the toxicant input rate function $h(x)$, we impose the following conditions:

(H) $h(x)\in C(\bar\Omega)$ and $h(x)\geq 0$

We first state the global existence and boundedness of solutions in the following theorem.

THEOREM 2.1 (global existence). *Let $\Omega\subset\mathbb{R}^2$ be a bounded domain with smooth boundary and the hypothesis (H) hold. Assume that $(u_0,w_0)\in[W^{1,p}(\Omega)]^2$ with $u_0,w_0\geq 0(\not\equiv 0)$ and $p>2$. Then system (2.1) has a unique global classical solution $(u,w)\in[C(\overline\Omega\times[0,\infty))\cap C^{2,1}(\overline\Omega\times(0,\infty))]^2$ satisfying $u,w>0$ for all $t>0$ and*

$$\|u(\cdot,t)\|_{L^\infty(\Omega)}+\|w(\cdot,t)\|_{W^{1,\infty}(\Omega)}\leq C, \tag{2.2}$$

where $C>0$ is a constant independent of t. In particular,

$$0<w\leq Q:=\max\{\|w_0\|_{L^\infty},\hat w\}, \tag{2.3}$$

where $\hat w:=\frac{\bar h}{g}$ with $\bar h:=\max_{x\in\bar\Omega}h(x)$.

Now, we assume that $h(x)\equiv h$ is a positive constant, which leads to the following system:

$$\begin{cases} u_t = d_1\Delta u+\chi\nabla\cdot(u\nabla w)+u(r-mw)-au^2, & x\in\Omega,\ t>0,\\ w_t = d_2\Delta w+h-gw-buw, & x\in\Omega,\ t>0,\\ \dfrac{\partial u}{\partial\nu}=\dfrac{\partial w}{\partial\nu}=0, & x\in\partial\Omega,\ t>0,\\ u(x,0)=u_0(x)\geq\not\equiv 0, w(x,0)=w_0(x)\geq\not\equiv 0, & x\in\Omega. \end{cases} \tag{2.4}$$

Then the conclusions of Theorem 2.1 hold true for (2.4) with

$$0<w\leq\bar Q:=\max\{\|w_0\|_{L^\infty},\overline{w}\}, \tag{2.5}$$

where $\overline{w}:=\frac{h}{g}$.

The next result is about the global stability of spatially homogeneous steady states of model (2.4), which satisfies the corresponding ODEs

$$\begin{cases} \dfrac{du}{dt}=u(r-au-mw),\\ \dfrac{dw}{dt}=h-buw-gw. \end{cases} \tag{2.6}$$

We may write the reaction term in the first equation of (2.4) as

$$u(r - au - mw) = ru\left(1 - \frac{u}{k}\right) - muw,$$

where $k := r/a$ is called the carrying capacity (i.e., the maximum population size of species that can be sustained by the environment). In what follows for the sake of simplicity the following notation will be frequently used:

$$\begin{aligned} &k := \frac{r}{a},\ k_0 := \frac{(\sqrt{2}-1)g}{b},\ k_1 := \frac{g}{b},\ h_1 := \frac{gr}{m}, \\ &h_2 := \frac{(ag+br)^2}{4abm},\ h_3 := \frac{2agr + br^2}{am},\ \hat{h}_1 := \frac{ag^2}{bm}. \end{aligned} \tag{2.7}$$

Then it is straightforward to check that the ODE system (2.6) has the following three possible constant solutions:

$$\begin{aligned} &(0,\overline{w}) := \left(0, \frac{h}{g}\right),\ (u^*,w^*) := \left(\frac{br - ag + \sqrt{\Delta}}{2ab}, \frac{h}{bu^* + g}\right), \\ &(u_*,w_*) := \left(\frac{br - ag - \sqrt{\Delta}}{2ab}, \frac{h}{bu_* + g}\right), \end{aligned} \tag{2.8}$$

where $\Delta = (ag+br)^2 - 4abmh \geq 0$ (i.e., $h \leq h_2$). The toxicant-only equilibrium $(0,\overline{w})$ always exists, while the coexistence equilibria (u_*,w_*) and (u^*,w^*) conditionally exist as specified below:

$$\begin{cases} (u^*,w^*) \text{ exists} & \text{only if either } h < h_1 \text{ or } k > k_1 \text{ and } h_1 \leq h \leq h_2, \\ (u_*,w_*) \text{ exists} & \text{only if } k > k_1 \text{ and } h_1 < h \leq h_2, \end{cases} \tag{2.9}$$

where $(u_*,w_*) = (u^*,w^*)$ when $k > k_1, h = h_2$. By elementary methods and calculations, one can easily obtain the stability (local or global) results of these equilibria. We summarize the stability results in Table 2.2 and postpone the proof to Appendix A.

Remark 2.1. Among various parameters in the model (2.4), in what follows, we shall explore how the global dynamics is related to the carrying capacity k and input rate h by fixing other parameters. Then we rewrite some constants defined in (2.7) in terms of k as follows:

$$h_1 = \frac{agk}{m}, h_2 = \frac{a(g+bk)^2}{4bm}, h_3 = \frac{2agk + abk^2}{m}, \hat{h}_1 = \frac{rg^2}{bmk}.$$

One can easily check that $h_1 \leq h_2$ for any $k > 0$, where $h_1 = h_2$ iff $k = k_1$. Furthermore $\hat{h}_1 = h_3$ iff $k = (\sqrt{2}-1)k_1 = k_0$, and $\hat{h}_1 > h_3$ if $k < k_0$ while $\hat{h}_1 < h_3$ if $k > k_0$. Fixing all parameters except k, we depict the graphs of these quantities in terms of k in Figure 2.1.

Table 2.2

Stability of the equilibria of the ODE system (2.6), *where* $k = k_1 \Leftrightarrow h_1 = h_2$ *and* LAS = *locally asymptotically stable,* GAS = *global asymptotically stable,* US = *unstable,* MS = *marginally stable.*

	$h < h_1$	$h = h_1$	$h_1 < h < h_2$	$h = h_2$	$h > h_2$
$k > k_1$	$(0,\overline{w}) : US$ $(u^*,w^*) : GAS$	$(0,\overline{w}) : MS$ $(u^*,w^*) : LAS$	$(0,\overline{w}) : LAS$ $(u^*,w^*) : LAS$ $(u_*,w_*) : US$	$(0,\overline{w}) : LAS$ $(u_*,w_*) =$ $(u^*,w^*) : MS$	$(0,\overline{w}) : GAS$
$k = k_1$		$(0,\overline{w}) : MS$	not applicable	$(0,\overline{w}) : MS$	
$k < k_1$			$(0,\overline{w}) : GAS$	$(0,\overline{w}) : GAS$	

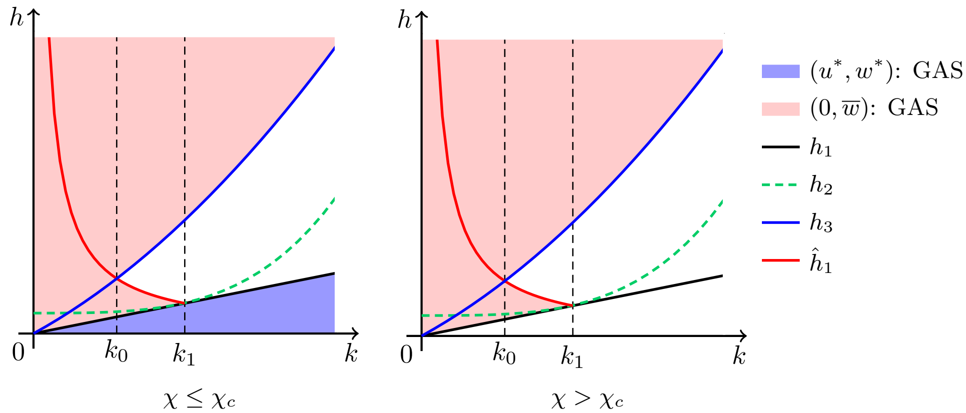

FIG. 2.1. *A schematic of global stability regions for the toxicant-only equilibrium* $(0, \overline{w})$ *and the coexistence equilibrium* (u^*, w^*).

We are now ready to state the results of global stability of the spatially uniform toxicant-only steady state $(0, \overline{w})$ and coexistence steady state (u^*, w^*) for the model (2.4), which will be proved in section 5 by using the Lyapunov functional method and LaSalle's invariant principle.

THEOREM 2.2 (global stability). *Assume that the assumptions in Theorem* 2.1 *hold and* $(u(x,t), w(x,t))$ *is the solution of* (2.4) *obtained in Theorem* 2.1. *Let* k_1, h_i $(i = 1, 2, 3)$ *and* $\hat{h}_1$ *be defined in* (2.7). *Then the following results hold:*

(i) *If the model parameters satisfy* $h > h_3$ *or*

$$0 < k \le k_1 \quad \text{and} \quad \begin{cases} h_1 < h \le h_3 & \text{if } k < (\sqrt{2}-1)k_1, \\ h_1 < h < \hat{h}_1 & \text{if } (\sqrt{2}-1)k_1 \le k < k_1, \end{cases} \tag{2.10}$$

then the steady state $(0, \overline{w})$ *is globally asymptotically stable. Moreover, there exist positive constants* $C_1 > 0$, $\lambda_1 > 0$, *and* $t_1 > 0$ *such that*

$$\|u\|_{L^\infty} + \|w - \overline{w}\|_{L^\infty} \le C_1 e^{-\lambda_1 t} \quad \text{for all } t > t_1. \tag{2.11}$$

(ii) *If* $h < h_1$, *then the coexistence steady state* (u^*, w^*) *is globally asymptotically stable provided that*

$$0 < \chi \le \chi_c := \sqrt{\frac{4md_1d_2(br + ag + \sqrt{\Delta})}{h(br - ag + \sqrt{\Delta})}} \tag{2.12}$$

with $\Delta = (ag + br)^2 - 4abmh$. *Moreover, there exist constants* $C_2 > 0$, $\lambda_2 > 0$, *and* $t_2 > 0$ *such that*

$$\|u - u^*\|_{L^\infty} + \|w - w^*\|_{L^\infty} \le C_2 e^{-\lambda_2 t} \quad \text{for all } t > t_2. \tag{2.13}$$

Due to the technical obstacles, we are unable to prove global stability results for the PDE model (2.4) as complete as those for the corresponding ODE system summarized in Table 2.2. For the convenience of comparison, we plot the parameter regimes for the global stability of constant steady states $(0, \overline{w})$ and (u^*, w^*) in Figure 2.1 indicated by the shaded regions, where $h_2 < h_3$ if $k > k_1$. This indicates that the pattern formation can only be possible when parameter values fall outside the shaded regions of Figure 2.1. In section 5, we shall perform linear stability analysis to identify the possible pattern formation parameter regimes as $\chi > 0$ is large and numerically illustrate the generated patterns along with their biological implications.

3. Global existence (proof of Theorem 2.1). The global existence of solutions consists of two parts: local existence and a priori estimates. In what follows, we shall use C or $C_i\,(i = 1, 2, \cdots)$ to denote a generic positive constant which may vary in context. Below we first give the local-in-time existence of classical solutions of problem (2.1) proved by the abstract theory of quasilinear parabolic systems in [3, 4].

LEMMA 3.1 (local existence with extension criterion). *Let $\Omega \subset \mathbb{R}^2$ be a bounded domain with smooth boundary and the hypothesis* (H) *hold. Assume $(u_0, w_0) \in [W^{1,p}(\Omega)]^2$ for $p > 2$ and $u_0, w_0 \geq 0 (\not\equiv 0)$. Then there exists a constant $T_{\max} > 0$ such that the problem* (2.1) *has a unique classical solution $(u, w) \in [C(\overline{\Omega} \times [0, T_{max})) \cap C^{2,1}(\overline{\Omega} \times (0, T_{max}))]^2$ satisfying $u, w > 0$ for all $t \in (0, T_{max})$ and the following extension criterion:*

$$\text{either}\, T_{\max} = \infty \text{ or } \lim_{t \nearrow T_{\max}} (\|u(\cdot, t)\|_{L^\infty} + \|w(\cdot, t)\|_{L^\infty}) = \infty. \tag{3.1}$$

Proof. With $\mathbb{V} = (u, w)$, the system (2.1) can be rewritten as

$$\begin{cases} \mathbb{V}_t = \nabla \cdot (B(\mathbb{V})\nabla\mathbb{V}) + \Phi(\mathbb{V}), & x \in \Omega,\ t \in (0, \mathrm{T}_{\max}), \\ \dfrac{\partial \mathbb{V}}{\partial \nu} = 0, & x \in \partial\Omega,\ t \in (0, \mathrm{T}_{\max}), \\ \mathbb{V}(\cdot, 0) = (u_0, w_0), & x \in \Omega, \end{cases} \tag{3.2}$$

where

$$B(\mathbb{V}) = \begin{bmatrix} d_1 & \chi u \\ 0 & d_2 \end{bmatrix},\ \Phi(\mathbb{V}) = \begin{bmatrix} u(r - au - mw) \\ h(x) - buw - gw \end{bmatrix}.$$

Clearly the matrix $B(\mathbb{V})$ is positive-definite, which indicates that (3.2) is normally parabolic. It follows from [3, Theorem 7.3] that there exists a $T_{\max} > 0$ such that the system (2.1) possesses a unique solution $(u, w) \in [C(\overline{\Omega} \times [0, \mathrm{T}_{\max})) \cap C^{2,1}(\overline{\Omega} \times (0, \mathrm{T}_{\max}))]^2$. Next, we show that $u(x, t) > 0$ for all $t \in (0, \mathrm{T}_{\max})$ by the maximum principle. To that end, we rewrite the first equation of (2.1) as

$$u_t = d_1 \Delta u + \chi \nabla u \cdot \nabla w + \chi u \Delta w + u(r - au - mw). \tag{3.3}$$

Hence, we assert that $u > 0$ for all $(x, t) \in \Omega \times (0, T_{\max})$ due to $u_0 \not\equiv 0$ by using the strong maximum principle. In the same way, we can get that $w > 0$ for all $(x, t) \in \Omega \times (0, T_{\max})$ by the strong maximum principle applied to the second equation of (2.1). Since $B(\mathbb{V})$ is an upper triangular matrix, the assertion (3.1) follows from [2, Theorem 5.2] directly. This completes the proof. ∎

Next, we are devoted to deriving the a priori estimates needed in the extension criterion of Lemma 3.1 to extend local solutions to global ones. To this end, we first derive some basic properties of solutions to system (2.1).

LEMMA 3.2. *Under the assumptions in Theorem* 2.1*, the solution of* (2.1) *satisfies*

$$w(x, t) \leq \max\{\|w_0\|_{L^\infty}, \hat{w}\} := Q \text{ for all } x \in \overline{\Omega} \text{ and } t > 0, \tag{3.4}$$

where $\hat{w}$ is defined by Theorem 2.1.

Proof. Noticing that $u, w > 0$ for all $t > 0$, we can show the above result by a comparison principle applied to the second equation of (2.1) and omit the proof for brevity. ∎

LEMMA 3.3. *Let the conditions in Lemma* 3.1 *hold and let* (u,w) *be a solution of system* (2.1). *Then there exists a constant* $C > 0$ *independent of* t *such that*

$$\|u(\cdot,t)\|_{L^1} \le C \quad \text{for all } t \in (0, T_{\max}), \tag{3.5}$$

and

$$\int_t^{t+\tau}\int_\Omega u^2 dxds \le C \text{ for all } t \in (0, T_{\max}-\tau), \tag{3.6}$$

where τ *is a constant such that*

$$0 < \tau < \min\{1, T_{\max}\}. \tag{3.7}$$

Proof. Integrating the first equation of (2.1) over Ω alongside the integration by parts and Young's inequality with $0 < w(x,t) \le Q$, we have

$$\begin{aligned} \frac{d}{dt}\int_\Omega udx + \int_\Omega udx &= \int_\Omega (r+1)udx - a\int_\Omega u^2dx - m\int_\Omega wudx \\ &\le (r+1+mQ)\int_\Omega udx - a\int_\Omega u^2dx \\ &\le \int_\Omega \left[\frac{au^2}{2} + \frac{(r+1+mQ)^2}{2a}\right]dx - a\int_\Omega u^2dx, \end{aligned} \tag{3.8}$$

and then

$$\frac{d}{dt}\int_\Omega udx + \int_\Omega udx + \frac{a}{2}\int_\Omega u^2dx \le C_1 := \frac{(r+1+mQ)^2|\Omega|}{2a}, \tag{3.9}$$

where $|\Omega|$ denotes the measure of Ω. Then we obtain (3.5) by the Gronwall inequality. Finally integrating (3.9) over $(t, t+\tau)$ yields (3.6) directly. ∎

Regarding the solution component w, we have the following a priori estimates.

LEMMA 3.4. *Let the conditions in Lemma* 3.1 *hold, and let* (u,w) *be a solution of the system* (2.1). *Then there exists a positive constant* $C > 0$ *such that*

$$\|\nabla w\|_{L^2} \le C \text{ for all } t \in (0, T_{\max}) \tag{3.10}$$

and

$$\int_t^{t+\tau}\int_\Omega |\Delta w|^2 dxds \le C \text{ for all } t \in (0, T_{\max}-\tau), \tag{3.11}$$

where τ *is given by* (3.7).

Proof. Multiplying the second equation of system (2.1) by w, integrating the result by parts, and recalling $\bar{h} = \max_{x\in\bar{\Omega}} h(x)$ and (3.4), we have

$$\frac{1}{2}\frac{d}{dt}\int_\Omega w^2dx + d_2\int_\Omega |\nabla w|^2dx = \int_\Omega (h(x) - buw - gw)wdx \le \int_\Omega \bar{h}wdx \le \bar{h}Q|\Omega|. \tag{3.12}$$

Integrating (3.12) over $(t, t+\tau)$, we get

$$\int_t^{t+\tau}\int_\Omega |\nabla w|^2 dxds \le \frac{1}{2d_2}\int_\Omega w^2 dx + \frac{\bar{h}Q|\Omega|\tau}{d_2} \le C_1 \text{ for all } t\in(0,\widetilde{T}_{\max}), \tag{3.13}$$

where $C_1 = \frac{Q^2|\Omega|+2\bar{h}Q|\Omega|\tau}{2d_2}$. Multiplying the second equation of system (2.1) by $-\Delta w$, integrating the result by parts, and using Young's inequality and (3.4), one has

$$\begin{aligned}\frac{1}{2}\frac{d}{dt}\int_\Omega |\nabla w|^2 dx + d_2\int_\Omega |\Delta w|^2 dx &= \int_\Omega (-h(x) + buw + gw)\Delta w dx\\ &\le \int_\Omega (\bar{h} + buw + gw)|\Delta w| dx\\ &\le \frac{d_2}{2}\int_\Omega |\Delta w|^2 dx + \frac{3b^2Q^2}{2d_2}\int_\Omega u^2 dx + C_2,\end{aligned} \tag{3.14}$$

where $C_2 = \frac{3|\Omega|}{2d_2}(\bar{h}^2 + g^2Q^2)$. This immediately gives

$$\frac{d}{dt}\int_\Omega |\nabla w|^2 dx + d_2\int_\Omega |\Delta w|^2 dx \le \frac{3b^2Q^2}{d_2}\int_\Omega u^2 dx + 2C_2, \tag{3.15}$$

which implies

$$\frac{d}{dt}\int_\Omega |\nabla w|^2 dx \le \int_\Omega |\nabla w|^2 dx + \frac{3b^2Q^2}{d_2}\int_\Omega u^2 dx + 2C_2.$$

Then with (3.6) and (3.13), one may obtain (3.10) by applying the uniform Gronwall inequality [35, Lemma III1.1] to the above inequality. Integrating (3.15) over $(t, t+\tau)$ along with (3.6) and (3.10), we get (3.11) and complete the proof of Lemma 3.4. $\square$

LEMMA 3.5. *Let the conditions in Lemma* 3.1 *hold. Then there exists a constant* $C > 0$ *independent of* t *such that*

$$\|u(\cdot,t)\|_{L^2} \le C \textit{ for all } t\in(0,T_{\max}). \tag{3.16}$$

Proof. Multiplying the first equation of (2.1) by $2u$ and integrating the result with respect to x over Ω alongside Young's inequality and the Hölder inequality, we have

$$\begin{aligned}&\frac{d}{dt}\int_\Omega u^2 dx + 2d_1\int_\Omega |\nabla u|^2 dx + 2a\int_\Omega u^3 dx\\ &\quad = -2\chi\int_\Omega u\nabla u\cdot\nabla w dx + 2r\int_\Omega u^2 dx - 2m\int_\Omega u^2 w dx\\ &\quad \le 2\int_\Omega \left(\frac{d_1|\nabla u|^2}{2} + \frac{\chi^2 u^2|\nabla w|^2}{2d_1}\right) dx + 2r\int_\Omega u^2 dx\\ &\quad \le d_1\int_\Omega |\nabla u|^2 dx + \frac{\chi^2}{d_1}\|u\|_{L^4}^2\|\nabla w\|_{L^4}^2 + 2r\|u\|_{L^2}^2.\end{aligned} \tag{3.17}$$

Next we estimate the term $\|u\|_{L^4}^2\|\nabla w\|_{L^4}^2$. First one can use the Gagliardo–Nirenberg inequality to derive that

$$\|u\|_{L^4}^2 \le C_1(\|\nabla u\|_{L^2}\|u\|_{L^2} + \|u\|_{L^2}^2). \tag{3.18}$$

With (3.10), we apply the Gagliardo–Nirenberg inequality along with an inequality in [8, Lemma 1] to obtain

$$\|\nabla w\|_{L^4}^2 \le C_2(\|\Delta w\|_{L^2}\|\nabla w\|_{L^2} + \|\nabla w\|_{L^2}^2) \le C_3(\|\Delta w\|_{L^2} + 1). \tag{3.19}$$

From (3.18), (3.19), and Young's inequality, we get

$$\begin{aligned} \frac{\chi^2}{d_1}\|u\|_{L^4}^2\|\nabla w\|_{L^4}^2 &\le C_4(\|\nabla u\|_{L^2}\|u\|_{L^2} + \|u\|_{L^2}^2)(\|\Delta w\|_{L^2} + 1) \\ &= C_4(\|\nabla u\|_{L^2}\|u\|_{L^2}\|\Delta w\|_{L^2} + \|\nabla u\|_{L^2}\|u\|_{L^2} \\ &\quad + \|u\|_{L^2}^2\|\Delta w\|_{L^2} + \|u\|_{L^2}^2) \\ &\le d_1\|\nabla u\|_{L^2}^2 + \frac{C_4^2}{d_1}\|u\|_{L^2}^2\|\Delta w\|_{L^2}^2 + C_5\|u\|_{L^2}^2 \end{aligned} \tag{3.20}$$

with $C_4 = \frac{\chi^2 C_1 C_3}{d_1}$ and $C_5 = \frac{C_4^2 + d_1^2 + 2C_4 d_1}{2d_1}$. Substituting (3.20) into (3.17), we obtain

$$\frac{d}{dt}\|u\|_{L^2}^2 \le \frac{C_4^2}{d_1}\|u\|_{L^2}^2\|\Delta w\|_{L^2}^2 + (2r + C_5)\|u\|_{L^2}^2 \le C_6\|u\|_{L^2}^2(\|\Delta w\|_{L^2}^2 + 1) \tag{3.21}$$

with $C_6 = \max\{\frac{C_4^2}{d_1}, 2r + C_5\}$, which yields (3.16) by the uniform Gronwall lemma [35, Lemma III1.1] and (3.11). This completes the proof of Lemma 3.5. ∎

Now we are in a position to derive the uniform estimate for $\|u(\cdot,t)\|_{L^\infty}$.

LEMMA 3.6. *Let the conditions in Lemma* 3.1 *hold. Then there exists a positive constant* $C > 0$ *independent of* t *such that*

$$\|u(\cdot,t)\|_{L^\infty} \le C \ \text{for all } t \in (0, T_{\max}). \tag{3.22}$$

Proof. We first show that if $\|u(\cdot,t)\|_{L^p} \le M (p \ge 1)$, then it follows that

$$\|\nabla w(\cdot,t)\|_{L^q} \le C_1 \ \text{ for all } t \in (0, T_{\max}) \tag{3.23}$$

with

$$q \in \begin{cases} [1, \frac{np}{n-p}) & \text{if } p < n, \\ [1, \infty) & \text{if } p = n, \\ [1, \infty] & \text{if } p > n. \end{cases} \tag{3.24}$$

Indeed, it follows from the second equation of (2.1) that w solves the following problem

$$w_t = d_2\Delta w - w + K(u,w) \ \text{in } \Omega, \ \frac{\partial w}{\partial \nu} = 0, \tag{3.25}$$

where $K(u,w) := w(1 - g - bu) + h(x)$. We have from (3.4) that

$$\|K(u,w)\|_{L^p} \le C_2(\|u\|_{L^p} + 1) \le C_2(M + 1) := C_3. \tag{3.26}$$

Hence, by the results of [23, Lemma 1] to the problem (3.25) with (3.26), we have (3.23) with (3.24).

Next we show that there is a constant $c > 0$ independent of t such that $\|u\|_{L^p} \le c$ for $p > 2$. Multiplying the first equation of (2.1) by u^{p-1} with $p > 2$ and integrating the result by parts, we have

$$\begin{aligned} &\frac{1}{p}\frac{d}{dt}\int_\Omega u^p dx + d_1(p-1)\int_\Omega u^{p-2}|\nabla u|^2 dx + a\int_\Omega u^{p+1} dx \\ &\quad = -(p-1)\chi\int_\Omega u^{p-1}\nabla u \cdot \nabla w dx + r\int_\Omega u^p dx - m\int_\Omega u^p w dx. \end{aligned} \tag{3.27}$$

Applying Young's inequality, we update (3.27) as

$$
\begin{aligned}
&\frac{1}{p}\frac{d}{dt}\int_\Omega u^p dx + d_1(p-1)\int_\Omega u^{p-2}|\nabla u|^2 dx + \int_\Omega u^p dx \\
&\le (p-1)\chi\int_\Omega u^{p-1}|\nabla u||\nabla w|dx + (r+1)\int_\Omega u^p dx \\
&\le \frac{d_1(p-1)}{2}\int_\Omega u^{p-2}|\nabla u|^2 dx + \frac{\chi^2(p-1)}{2d_1}\int_\Omega u^p|\nabla w|^2 dx + (r+1)\int_\Omega u^p dx.
\end{aligned}
\tag{3.28}
$$

Noting that $\int_\Omega u^{p-2}|\nabla u|^2 dx = \frac{4}{p^2}\int_\Omega |\nabla u^{\frac{p}{2}}|^2 dx$, one derives that

$$
\begin{aligned}
&\frac{d}{dt}\int_\Omega u^p dx + \frac{2d_1(p-1)}{p}\int_\Omega |\nabla u^{\frac{p}{2}}|^2 dx + p\int_\Omega u^p dx \\
&\quad\le \frac{\chi^2 p(p-1)}{2d_1}\int_\Omega u^p|\nabla w|^2 dx + p(r+1)\int_\Omega u^p dx
\end{aligned}
\tag{3.29}
$$

for all $t \in (0, T_{\max})$ and $p > 2$. It follows from Lemma 3.5 that $\|u^{\frac{p}{2}}(\cdot,t)\|_{L^{\frac{4}{p}}} = \|u(\cdot,t)\|_{L^2}^{\frac{p}{2}} \le C^{\frac{p}{2}}$, and hence $\|\nabla w\|_{L^4} \le C_4$ by using (3.23). Employing the Hölder inequality, the Gagliardo–Nirenberg inequality and Young's inequality, one derives that

$$
\begin{aligned}
\frac{\chi^2 p(p-1)}{2d_1}\int_\Omega u^p|\nabla w|^2 dx &\le \frac{\chi^2 p(p-1)}{2d_1}\left(\int_\Omega u^{2p}dx\right)^{\frac{1}{2}}\left(\int_\Omega |\nabla w|^4 dx\right)^{\frac{1}{2}} \\
&\le \frac{\chi^2 p(p-1)C_4^2}{2d_1}\|u^{\frac{p}{2}}\|_{L^4}^2 \\
&\le C_5\left(\|\nabla u^{\frac{p}{2}}\|_{L^2}^{2(1-\frac{1}{p})}\|u^{\frac{p}{2}}\|_{L^{\frac{4}{p}}}^{\frac{2}{p}} + \|u^{\frac{p}{2}}\|_{L^{\frac{4}{p}}}^2\right) \\
&\le C_5 C\|\nabla u^{\frac{p}{2}}\|_{L^2}^{2(1-\frac{1}{p})} + C_5 C^p \\
&\le \frac{(p-1)d_1}{p}\|\nabla u^{\frac{p}{2}}\|_{L^2}^2 + \frac{d_1}{p}\left(\frac{C_5 C}{d_1}\right)^p + C_5 C^p.
\end{aligned}
\tag{3.30}
$$

Similarly, by the Gagliardo–Nirenberg inequality and Young's inequality, we have

$$
\begin{aligned}
p(r+1)\int_\Omega u^p dx &= p(r+1)\|u^{\frac{p}{2}}\|_{L^2}^2 \\
&\le C_6\left(\|\nabla u^{\frac{p}{2}}\|_{L^2}^{2(1-\frac{2}{p})}\|u^{\frac{p}{2}}\|_{L^{\frac{4}{p}}}^{\frac{4}{p}} + \|u^{\frac{p}{2}}\|_{L^{\frac{4}{p}}}^2\right) \\
&\le C_6 C^2\|\nabla u^{\frac{p}{2}}\|_{L^2}^{2(1-\frac{2}{p})} + C_6 C^p \\
&\le \frac{(p-1)d_1}{p}\|\nabla u^{\frac{p}{2}}\|_{L^2}^2 + \frac{2}{p}\left[\frac{d_1(p-1)}{p-2}\right]^{\frac{2-p}{2}}(C_6C^2)^{\frac{p}{2}} + C_6 C^p.
\end{aligned}
\tag{3.31}
$$

Substituting (3.30) and (3.31) into (3.29) gives

$$
\frac{d}{dt}\int_\Omega u^p dx + p\int_\Omega u^p dx \le C_7
$$

with $C_7 = \frac{d_1}{p}(\frac{C_5 C}{d_1})^p + \frac{2}{p}[\frac{d_1(p-1)}{p-2}]^{\frac{2-p}{2}}(C_6C^2)^{\frac{p}{2}} + (C_5 + C_6)C^p$. It follows from the Gronwall inequality that

$$
\|u(\cdot,t)\|_{L^p}^p \le e^{-pt}\|u_0\|_{L^p}^p + \frac{C_7}{p}(1-e^{-pt}) \le \|u_0\|_{L^p}^p + \frac{C_7}{p}.
\tag{3.32}
$$

Hence, choosing $p=4$ in (3.32) and using (3.23), we can find a constant $C_8>0$ such that

$$\|w(\cdot,t)\|_{W^{1,\infty}}\le C_8. \tag{3.33}$$

Noting (3.33), and applying the Cauchy–Schwarz inequality, we get from (3.27)

$$\begin{aligned}
\frac{1}{p}\frac{d}{dt}\int_\Omega u^p dx =& -\frac{4d_1(p-1)}{p^2}\int_\Omega |\nabla u^{\frac{p}{2}}|^2 dx-(p-1)\chi\int_\Omega u^{p-1}\nabla u\cdot\nabla w dx\\
&+r\int_\Omega u^p dx-m\int_\Omega u^p w dx-a\int_\Omega u^{p+1}dx\\
\le& -\frac{4d_1(p-1)}{p^2}\int_\Omega |\nabla u^{\frac{p}{2}}|^2 dx+C_8(p-1)\chi\int_\Omega u^{p-1}|\nabla u|dx+r\int_\Omega u^p dx\\
=& -\frac{4d_1(p-1)}{p^2}\int_\Omega |\nabla u^{\frac{p}{2}}|^2 dx+\frac{2C_8(p-1)\chi}{p}\int_\Omega u^{\frac{p}{2}}|\nabla u^{\frac{p}{2}}|dx+r\int_\Omega u^p dx\\
\le& -\frac{2d_1(p-1)}{p^2}\int_\Omega |\nabla u^{\frac{p}{2}}|^2 dx+\left(\frac{C_8^2\chi^2}{2d_1}+r\right)(p-1)\int_\Omega u^p dx
\end{aligned}$$

for all $t\in(0,T_{\max})$. This further yields

$$\frac{d}{dt}\int_\Omega u^p dx+p(p-1)\int_\Omega u^p dx\le -\frac{2d_1(p-1)}{p}\int_\Omega |\nabla u^{\frac{p}{2}}|^2 dx+C_9 p(p-1)\int_\Omega u^p dx \tag{3.34}$$

for all $t\in(0,T_{\max})$ and $p>2$, where $C_9=\frac{C_8^2\chi^2}{2d_1}+r+1$. With (3.34), one can use the Moser–Alikakos iteration (see [1]) to derive (3.22). Since the procedure is routine, we omit the details for brevity and complete the proof. ∎

Proof of Theorem 2.1. The extension criterion in Lemma 3.1 with Lemma 3.6 immediately gives the global existence and boundedness of the solutions of system (2.1), namely Theorem 2.1. ∎

4. Global stability of solutions (proof of Theorem 2.2). In this section, we shall prove the global stability results in Theorem 2.2 by using Lyapunov functional method and LaSalle's invariant principle. We first present a basic following result.

LEMMA 4.1. *For positive constant $\tilde{w}$, we define a function*

$$\zeta(w)=w-\tilde{w}-\tilde{w}\ln\frac{w}{\tilde{w}}.$$

Then $\zeta(w)$ is a convex function such that $\zeta(w)\ge 0$ where "$=$" holds if and only if $w=\tilde{w}$. Furthermore, as $w\to\tilde{w}$, it holds that

$$c_1(w-\tilde{w})^2\le\zeta(w)\le c_2(w-\tilde{w})^2, \tag{4.1}$$

where $c_1=\frac{1}{4\tilde{w}}, c_2=\frac{1}{\tilde{w}}$.

Proof. Applying the Taylor expansion to $\zeta(w)$ gives the result directly. ∎

The following regularity results as a consequence of Schauder estimates will be used.

LEMMA 4.2. *Let (u,v,w) be the unique global bounded classical solution of* (2.4) *obtained in Theorem* 2.1. *Then for any given $0<\alpha<1$, there exists a constant $C>0$ such that*

$$\|u\|_{C^{2+\alpha,1+\frac{\alpha}{2}}(\bar{\Omega}\times[1,\infty))}+\|w\|_{C^{2+\alpha,1+\frac{\alpha}{2}}(\bar{\Omega}\times[1,\infty))}\le C. \tag{4.2}$$

Proof. The results are obtained by the parabolic regularity theory (cf. [30, Theorem 1.3]) and standard parabolic Schauder theory (cf. [24]). The proof details can follow the same way as the proof of [37, Lemma 3.4], and details are omitted for brevity. ∎

Proof of Theorem 2.2 (i). We first prove the global stability of $(0,\overline{w})$ via the Lyapunov functional method and LaSalle's invariant principle [26] applied to infinite dimensional dynamical system (cf. [11, 31]) by interpreting the system (2.4) to an infinite dynamical system based on the compactness results given in Lemma 4.2. To this end, we rewrite the quasilinear system (2.4) as a form of semilinear parabolic system

$$
\begin{cases}
u_t = d_1\Delta u + u(r-mw) - au^2 + \phi(x,t), & x\in\Omega,\ t>0,\\
w_t = d_2\Delta w + h - gw - buw, & x\in\Omega,\ t>0,\\
\dfrac{\partial u}{\partial\nu} = \dfrac{\partial w}{\partial\nu} = 0, & x\in\partial\Omega,\ t>0,\\
u(x,0) = u_0(x) \geq\not\equiv 0, w(x,0) = w_0(x) \geq\not\equiv 0, & x\in\Omega,
\end{cases}
\tag{4.3}
$$

where $\phi(x,t) := \chi\nabla u\cdot\nabla w + u\Delta w$. For each initial value $y_0 = (u_0,w_0)$, we use $Y(t;y_0) = (u,w)(t)$ to denote the unique global classical solution of (2.4) (i.e., (4.3)) for $t>0$, which defines a semiflow on the Banach space $X = [W^{1,p}(\overline{\Omega})]^2$ with $p>2$ (see [2, 19]) from the global existence results in Theorem 2.1 and regularity results in Lemma 4.2. Now we define a functional

$$
G_1(u,w) = \alpha\int_\Omega u dx + \frac{\beta}{2}\int_\Omega (w-\bar{w})^2 dx,
\tag{4.4}
$$

where $\alpha,\beta>0$ are chosen appropriately for different cases as shown later. It is easy to find that $G_1(Y)=0$ iff $Y=(0,\overline{w})$ and $G_1(Y)>0$ for all $Y\neq(0,\overline{w})$, which implies that $G_1(Y)$ is a positive definite function. Moreover, by the definition of $G_1(Y)$ and the results of Theorem 2.1, we get $G_1(Y)\leq C_1$ for some constant $C_1>0$ independent of $t>0$.

Next, we prove $\frac{d}{dt}G_1(Y) := \frac{d}{dt}G_1(t)\leq 0$ for all $Y\in X$. Indeed, differentiating the functional (4.4) with respect to t, using the equations in (2.4) and the integration by parts, we have

$$
\begin{aligned}
\frac{d}{dt}G_1(t) &= \alpha\int_\Omega u_t dx + \beta\int_\Omega (w-\overline{w})w_t dx\\
&= \alpha\int_\Omega u(r-au-mw)dx + \beta\int_\Omega (w-\overline{w})\left(d_2\Delta w + h - buw - gw\right)dx\\
&= \int_\Omega [\alpha ru - \alpha au^2 - \alpha mu(w-\overline{w}) - \alpha m\overline{w}u]dx\\
&\quad + \beta\int_\Omega (w-\overline{w})(h-buw-gw)dx - \beta d_2\int_\Omega |\nabla w|^2 dx.
\end{aligned}
\tag{4.5}
$$

Next we proceed with two cases.

Case 1: $h>h_3$. In this case, from the definition of h_3 in (2.7), we see that $h>h_3>\frac{2gr}{m}$. Let $\alpha = b\overline{w}^2, \beta = m\overline{w}-2r = \frac{mh-2gr}{g}>0$. Straightforward calculations give us that

$$
\begin{aligned}
\frac{d}{dt}G_1(t) &= \int_\Omega [-\alpha a u^2 - (\alpha m - \beta b\overline{w})u(w-\overline{w}) - \beta g(w-\overline{w})^2]dx \\
&\quad - \int_\Omega (\alpha m\overline{w} - \alpha r - \beta b\overline{w}^2)udx - \int_\Omega \beta b u w^2 dx - \beta d_2 \int_\Omega |\nabla w|^2 dx \\
&= \int_\Omega [-ab\overline{w}^2u^2 - 2br\overline{w}u(w-\overline{w}) - (m\overline{w}-2r)g(w-\overline{w})^2]dx \\
&\quad - br\overline{w}^2\int_\Omega udx - (m\overline{w}-2r)\left(b\int_\Omega uw^2dx + d_2\int_\Omega |\nabla w|^2dx\right) \\
&= -\int_\Omega \Theta^T A_1 \Theta dx - br\overline{w}^2\int_\Omega udx \\
&\quad - (m\overline{w}-2r)\left(b\int_\Omega uw^2dx + d_2\int_\Omega |\nabla w|^2dx\right),
\end{aligned}
\tag{4.6}
$$

where Θ^T denotes the transpose of Θ and

$$
\Theta = \begin{bmatrix} u \\ w-\overline{w} \end{bmatrix},\ A_1 = \begin{bmatrix} ab\overline{w}^2 & br\overline{w} \\ br\overline{w} & (m\overline{w}-2r)g \end{bmatrix}.
\tag{4.7}
$$

One can directly check that $m\overline{w}-2r>0$, and hence the matrix A_1 is positive definite if $h>h_3$. Then $\frac{d}{dt}G_1(t)\le 0$ for all $t>0$ if $h>h_3$, where $\frac{d}{dt}G_1(t)=0$ iff $Y=(0,\overline{w})$ from (4.6). Due to the results in Lemma 4.2, we see that $\phi(x,t)$ is uniformly bounded in $\bar\Omega\times[1,\infty)$. Therefore the Lyapunov function method for PDEs and the LaSalle invariant principle in the Banach space $X=[W^{1,p}(\overline{\Omega})]^2$ with $p>2$ (cf. [11, 31]) assert that the trajectory $Y(t;y_0)=(u,w)\to(0,\overline{w})$ in X as $t\to\infty$ and hence $(0,\overline{w})$ is globally asymptotically stable in L^∞-topology by the Sobolev embedding inequality along with Lemma 4.2.

Case 2: $h\le h_3$. Let $\alpha=\frac{\overline{w}}{m}, \beta=\frac{1}{b}$. Simple calculation yields

$$
\begin{aligned}
\frac{d}{dt}G_1(t) &= \int_\Omega [-\alpha a u^2 - (\alpha m + \beta b\overline{w})u(w-\overline{w}) - \beta g(w-\overline{w})^2]dx \\
&\quad - \int_\Omega \alpha(m\overline{w}-r)udx - \int_\Omega \beta bu(w-\overline{w})^2dx - \beta d_2\int_\Omega |\nabla w|^2dx \\
&= -\int_\Omega \Theta^T A_2\Theta dx - \frac{h(mh-gr)}{mg^2}\int_\Omega udx - \int_\Omega u(w-\overline{w})^2dx \\
&\quad - \frac{d_2}{b}\int_\Omega |\nabla w|^2dx,
\end{aligned}
\tag{4.8}
$$

where Θ is as defined in (4.7) and

$$
A_2 = \begin{bmatrix} \dfrac{a\overline{w}}{m} & \overline{w} \\ \overline{w} & \dfrac{g}{b} \end{bmatrix}.
$$

It is clear that $mh-gr>0$ iff $h>h_1$, and the matrix A_2 is positive definite iff $h<\hat h_1$. Noticing that $h_1<h_3$ and $h_1\le\hat h_1$ if $0<k\le k_1$ where

$$
\begin{cases} \hat h_1 > h_3 & \text{if } k<k_0, \\ \hat h_1 \le h_3 & \text{if } k\ge k_0, \end{cases}
$$

with $k_0=(\sqrt{2}-1)k_1<k_1$, and $\hat h_1<h_1$ iff $k>k_1$, we have from (4.8) that $\frac{d}{dt}G_1(t)\le 0$ for all $t>0$ if (2.10) is satisfied, where $\frac{d}{dt}G_1(t)=0$ iff $Y=(0,\overline{w})$. By the same argument as above, we get that $(0,\overline{w})$ is globally asymptotically stable.

We proceed to derive the convergence rate of solutions. Indeed, from the above analysis shown in Case 1 and Case 2, for $h > h_3$ or (2.10), we can find a positive constant C_2 such that

$$\frac{d}{dt}G_1(t) \leq -C_2 G_1(t) \text{ for all } t > 0. \tag{4.9}$$

Then solving the above inequality gives $G_1(t) \leq C_3 e^{-C_4 t}$ for all $t > 0$ for some constants $C_3, C_4 > 0$. This along with (4.4) shows that

$$\|u\|_{L^1} + \|w - \overline{w}\|_{L^2} \leq C_5 e^{-C_4 t} \text{ for all } t > 0. \tag{4.10}$$

Next we proceed to derive the decay rates of L^∞-norm. It follows from Theorem 2.1 that $\chi u \nabla w$ and $u(r - au - mw)$ are bounded in $L^\infty(\Omega \times (0, \infty))$. The results of Lemma 4.2 yield a positive constant $C_6 > 0$ such that

$$\|u\|_{W^{1,\infty}} \leq C_6 \text{ for all } t > 1.$$

Then from the Gagliardo–Nirenberg inequality and (4.10), we get

$$\|u\|_{L^\infty} \leq C_7 \left(\|\nabla u\|_{L^\infty}^{\frac{2}{3}} \|u\|_{L^1}^{\frac{1}{3}} + \|u\|_{L^1} \right) \leq C_8 \left(\|u\|_{L^1}^{\frac{1}{3}} + \|u\|_{L^1} \right) \leq C_9 e^{-C_{10} t} \tag{4.11}$$

for $t > t_1$ with some $t_1 > 1$. Moreover, from Theorem 2.1, we have $w - \overline{w} \in W^{1,\infty}(\Omega)$ due to $w \in W^{1,\infty}(\Omega)$. Thanks to the Gagliardo–Nirenberg inequality and (4.10), we obtain

$$\|w - \overline{w}\|_{L^\infty} \leq C_{11} \left(\|\nabla (w - \overline{w})\|_{L^\infty}^{\frac{1}{2}} \|w - \overline{w}\|_{L^2}^{\frac{1}{2}} + \|w - \overline{w}\|_{L^2} \right) \leq C_{12} e^{-C_{13} t} \tag{4.12}$$

for all $t > t_1$. Combining (4.11) and (4.12), we get (2.11) with $\lambda_1 = \min\{C_{10}, C_{13}\}$. $\square$

Proof of Theorem 2.2 (ii). Define the following Lyapunov functional:

$$G_2(u(t), w(t)) := G_2(t) = \Gamma_1 \int_\Omega \left(u - u^* - u^* \ln \frac{u}{u^*} \right) dx + \frac{\Gamma_2}{2} \int_\Omega (w - w^*)^2 dx, \tag{4.13}$$

where $\Gamma_1 := \frac{b}{m}$ and $\Gamma_2 := \frac{1}{w^*}$ are positive constants. Then it follows from Lemma 4.1 that $G_2(t) \geq 0$ for all $u, w > 0$ where "=" holds iff $u = u^*, w = w^*$. Next differentiating $G_2(t)$ with respect to t and using the equations in (2.4), one has

$$\frac{d}{dt}G_2(t) = \Gamma_1 \int_\Omega \left(1 - \frac{u^*}{u} \right) u_t dx + \Gamma_2 \int_\Omega (w - w^*) w_t dx := \ell_1 + \ell_2, \tag{4.14}$$

where

$$\ell_1 = -\Gamma_1 d_1 u^* \int_\Omega \left| \frac{\nabla u}{u} \right|^2 dx - \Gamma_1 \chi u^* \int_\Omega \frac{\nabla u \cdot \nabla w}{u} dx - \Gamma_2 d_2 \int_\Omega |\nabla w|^2 dx$$

and

$$\ell_2 = \Gamma_1 \int_\Omega \left(1 - \frac{u^*}{u} \right) (ru - au^2 - muw) dx + \Gamma_2 \int_\Omega (w - w^*)(h - buw - gw) dx.$$

Clearly ℓ_1 can be rewritten as

$$\ell_1 = -\int_\Omega \Theta^T A \Theta dx, \; \Theta = \begin{bmatrix} \nabla u \\ \nabla w \end{bmatrix}, \; A = \begin{bmatrix} \frac{\Gamma_1 d_1 u^*}{u^2} & \frac{\Gamma_1 \chi u^*}{2u} \\ \frac{\Gamma_1 \chi u^*}{2u} & \Gamma_2 d_2 \end{bmatrix}.$$

The matrix A is positive semidefinite (i.e., $\ell_1 \le 0$) iff $\frac{\Gamma_1\Gamma_2 d_1 d_2 u^*}{u^2} \ge \frac{\Gamma_1^2\chi^2(u^*)^2}{4u^2}$, which is equivalent to (2.12). Next, using the facts

$$\begin{cases} r - au^* - mw^* = 0, \\ h - bu^*w^* - gw^* = 0, \end{cases} \tag{4.15}$$

we can rearrange ℓ_2 as

$$\begin{aligned} \ell_2 &= -\Gamma_1 a \int_\Omega (u-u^*)^2 dx - (\Gamma_1 m + \Gamma_2 bw^*) \int_\Omega (u-u^*)(w-w^*) dx \\ &\quad - \Gamma_2 g \int_\Omega (w-w^*)^2 dx - \Gamma_2 b \int_\Omega u(w-w^*)^2 dx \\ &= -\int_\Omega \Lambda^T B \Lambda dx - \Gamma_2 b \int_\Omega u(w-w^*)^2 dx, \end{aligned} \tag{4.16}$$

where

$$\Lambda = \begin{bmatrix} u-u^* \\ w-w^* \end{bmatrix}, \; B = \begin{bmatrix} \Gamma_1 a & \dfrac{\Gamma_1 m + \Gamma_2 bw^*}{2} \\ \dfrac{\Gamma_1 m + \Gamma_2 bw^*}{2} & \Gamma_2 g \end{bmatrix}.$$

Since $\Gamma_1 a > 0$, the matrix B is positive definite iff

$$\mathrm{Det(B)} = \Gamma_1\Gamma_2 ag - \frac{(\Gamma_1 m + \Gamma_2 bw^*)^2}{4} = \frac{b(ag - bmw^*)}{mw^*} > 0,$$

namely $w^* < \frac{ag}{bm}$. By virtue of the definition and existence of w^* (see (2.8) and (2.9)), we see that $w^* < \frac{ag}{bm}$ if $h < h_1$. Then $\ell_2 < 0$ if $h < h_1$. Therefore, $\frac{d}{dt}G_2(t) \le 0$ for all $t > 0$ if $h < h_1$ and (2.12) holds, where $\frac{d}{dt}G_2(t) = 0$ iff $(u, w) = (u^*, w^*)$. Hence, (u^*, w^*) is globally asymptotically stable by the Lyapunov function method along with the LaSalle invariant principle and Lemma 4.2.

Next, we proceed to show the decay rate (2.13). First, by the Sylvester criterion, the fact that the matrix B is positive definite ensures a constant $\theta > 0$ such that $\Lambda^T B \Lambda \ge \theta|\Lambda|^2 = \theta[(u-u^*)^2 + (w-w^*)^2]$. Since A is positive semidefinite, there is a positive constant $C_1 > 0$ such that

$$\frac{d}{dt}G_2(t) \le -C_1 \int_\Omega \left[(u-u^*)^2 + (w-w^*)^2\right] dx. \tag{4.17}$$

Applying Lemma 4.1, we can find a $t_2 > 0$ such that for all $t > t_2$ the following inequality holds:

$$\frac{1}{4u^*}\int_\Omega (u-u^*)^2 dx \le \int_\Omega \left(u - u^* - u^* \ln\frac{u}{u^*}\right) dx \le \frac{1}{u^*}\int_\Omega (u-u^*)^2 dx. \tag{4.18}$$

Combining (4.13) with (4.18), we can find constants $C_2 > 0$ and $C_3 > 0$ such that

$$C_2\left(\|u-u^*\|_{L^2}^2 + \|w-w^*\|_{L^2}^2\right) \le G_2(t) \le C_3\left(\|u-u^*\|_{L^2}^2 + \|w-w^*\|_{L^2}^2\right)$$

for all $t > t_2$. Hence, one can find a constant $C_4 > 0$ such that

$$\frac{d}{dt}G_2(t) \le -C_4 G_2(t) \text{ for all } t > t_2, \tag{4.19}$$

which, by the Gronwall inequality, yields the exponential decay

$$\|u-u^*\|_{L^2}^2 + \|w-w^*\|_{L^2}^2 \le C_5 e^{-C_6 t}$$

for positive constants C_5 and C_6. Then we use a similar procedure as for (4.11) and (4.12) to finally obtain the exponential decay rate (2.13) and complete the proof of Theorem 2.2. ∎

5. Spatially inhomogeneous patterns. While Theorem 2.2 gives some parameter regimes (as illustrated in Figure 2.1) in which pattern formation (i.e., spatially inhomogeneous solutions) is impossible, a natural question is what may happen outside these stability regimes. In this section, we shall perform the linear instability analysis for the model (2.4) to show that patterns may bifurcate from the coexistence steady states in some parameter regimes. Moreover, we use numerical simulations to illustrate the patterns generated by the model (2.4) and discuss their biological implications.

5.1. Linear instability. Note that the stability of the equilibria of the ODE system has been summarized in Table 2.2. We shall examine under what conditions the stable equilibria of the ODE system will become unstable in the presence of spatial variables. To this end, we linearize the system (2.4) about a constant stable state (u_s, w_s) and obtain

$$\begin{cases} \Psi_t = \mathbf{A}\Delta\Psi + J\Psi, & x \in \Omega,\ t > 0, \\ \nabla\Psi \cdot \nu = 0, & x \in \partial\Omega,\ t > 0, \\ \Psi(\cdot, 0) = (u_0 - u_s, w_0 - w_s)^{\mathsf{T}}, & x \in \Omega, \end{cases} \tag{5.1}$$

where

$$\Psi = \begin{bmatrix} u - u_s \\ w - w_s \end{bmatrix},\ \mathbf{A} = \begin{bmatrix} d_1 & \chi u_s \\ 0 & d_2 \end{bmatrix},\ J = \begin{bmatrix} r - 2au_s - mw_s & -mu_s \\ -bw_s & -bu_s - g \end{bmatrix},$$

and T denotes the transpose. We let $0 = \lambda_0 < \lambda_1 \le \lambda_2 \le \cdots$ ($\lambda_\kappa \to +\infty$ as $\kappa \to \infty$) be the sequence of eigenvalues for the elliptic operator $-\Delta$ on Ω subject to the Neumann boundary condition on Ω, and we let $\varphi_\kappa(x)$ be the eigenfunctions corresponding to λ_κ, that is,

$$\begin{cases} \Delta\varphi_\kappa(x) + \lambda_\kappa\varphi_\kappa(x) = 0, & x \in \Omega, \\ \dfrac{\partial\varphi_\kappa(x)}{\partial\nu} = 0, & x \in \partial\Omega. \end{cases}$$

We then look for solutions of (5.1) of the form

$$\Psi_\kappa(x, t) = \begin{pmatrix} c_{1\kappa}\varphi_\kappa(x) \\ c_{2\kappa}\varphi_\kappa(x) \end{pmatrix} e^{\rho t}, \tag{5.2}$$

where the real numbers $c_{1\kappa}$ and $c_{2\kappa}$ are determined by the Fourier expansion of the initial conditions and ρ is the temporal eigenvalue. Thus, by the principle of superposition, the linear system (5.1) has the solution

$$\Psi(x, t) = \sum_{\kappa=0}^{\infty} \Psi_\kappa(x, t),$$

where κ is called the wave number.

Inserting (5.2) into (5.1) yields

$$I\rho\varphi_\kappa(x) = -\lambda_\kappa\mathbf{A}\varphi_\kappa(x) + J\varphi_\kappa(x),$$

which implies ρ is the eigenvalue of the following matrix:

$$M_\kappa := -\lambda_\kappa\mathbf{A} + J = \begin{bmatrix} -d_1\lambda_\kappa + r - 2au_s - mw_s & -\chi u_s\lambda_\kappa - mu_s \\ -bw_s & -d_2\lambda_\kappa - bu_s - g \end{bmatrix}.$$

Next we investigate whether the eigenvalues of the matrix M_κ at stable $(0,\overline{w})$ or (u^*,w^*) have positive real part, which depends on the sign of the trace and determinant of M_κ. One can easily check that when $h>h_1$, the eigenvalue ρ for the toxicant-only steady state $(0,\overline{w})$ has negative real part, and hence no bifurcation (i.e., no pattern formation) will arise from the equilibrium $(0,\overline{w})$. Therefore, the pattern formation (if any) can only arise from the coexistence steady state (u^*,w^*), which is stable if $h<h_1$ or $k>k_1$ and $h_1\le h<h_2$ in the ODE system (see Table 2.2).

At (u^*,w^*), we find that

$$\mathrm{Trace}(M_\kappa)=-(d_1+d_2)\lambda_\kappa-au^*-bu^*-g<0,$$

$$\mathrm{Det}(M_\kappa)=d_1d_2\lambda_\kappa^2+\beta_1\lambda_\kappa+\beta_2, \tag{5.3}$$

where

$$\beta_1:=d_1bu^*+d_1g+d_2au^*-\chi bu^*w^*,\quad \beta_2:=ab(u^*)^2+au^*g-mbu^*w^*.$$

Note that $\beta_2=\mathrm{Det}(J)>0$ since (u^*,w^*) is a stable equilibrium of ODE system (2.6). Thus, if $\beta_1\ge 0$ (i.e., $\chi\le\frac{d_1bu^*+d_1g+d_2au^*}{bu^*w^*}$), then $\mathrm{Det}(M_\kappa)>0$, and all eigenvalues of the matrix M_κ have negative real part, which indicates that (u^*,w^*) is linearly stable for the PDE system (2.4).

Next we consider the case where $\chi>\frac{d_1bu^*+d_1g+d_2au^*}{bu^*w^*}$ (i.e., $\beta_1<0$). By thinking of (5.3) as a quadratic equation with respect to λ_κ, one can easily find that if $\beta_1^2-4d_1d_2\beta_2>0$, which is equivalent to

$$\chi>\frac{2\sqrt{d_1d_2\beta_2}+d_1(bu^*+g)+d_2au^*}{bu^*w^*}:=\chi_b, \tag{5.4}$$

then $\mathrm{Det}(M_\kappa)$ has two values of λ_κ where it vanishes, namely,

$$\lambda_\pm:=\frac{-\beta_1\pm\sqrt{\beta_1^2-4d_1d_2\beta_2}}{2d_1d_2},$$

and $\mathrm{Det}(M_\kappa)$ becomes negative when

$$\lambda_-<\lambda_\kappa<\lambda_+. \tag{5.5}$$

Note that $0<\lambda_-<\lambda_+$ since $\beta_1<0,\beta_2>0$, and $\beta_1^2-4d_1d_2\beta_2>0$. Therefore, if the conditions (5.4) and (5.5) are satisfied, one of the eigenvalues of the matrix M_κ is a positive real number, and the homogeneous steady state (u^*,w^*) is unstable for the PDE system. Summarizing the above results, we have the following conclusions.

THEOREM 5.1. *Assume that the coexistence equilibrium* (u^*,w^*) *is locally asymptotically stable with respect to the ODE system* (2.6) *(i.e., the parameters satisfy either* $0<h<h_1$ *or* $k>k_1$, $h_1\le h<h_2$*). Then*

(i) (u^*,w^*) *is linearly stable with respect to the reaction-diffusion system* (2.4) *if* $\chi<\chi_b$, *and*

(ii) (u^*,w^*) *is unstable with respect to the reaction-diffusion system* (2.4) *if both conditions* $\chi>\chi_b$ *and* $\lambda_-<\lambda_\kappa<\lambda_+$ *(for some* κ*) hold.*

Remark 5.1. From the expressions for χ_b and χ_c (see (2.12) and (5.4)), we cannot completely compare their sizes, but we can assert that $\chi_b>\chi_c$ if $h<\frac{12(ag+br)^2}{49abm}(<h_2)$.

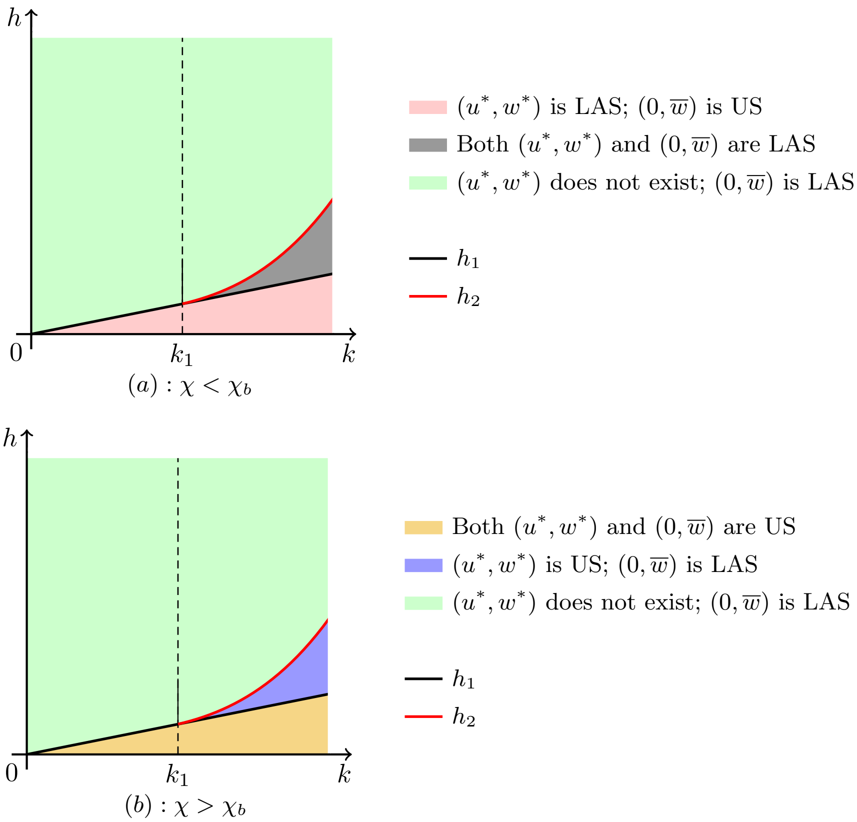

FIG. 5.1. *A schematic of local stability and instability regions for* $\chi < \chi_b$ *and* $\chi > \chi_b$.

Based on the linear stability results obtained above, we depict the local stability and instability regions in the (k, h) plane for model (2.4) in Figure 5.1.

5.2. Numerical simulations and applications. In this section, we numerically solve model (2.4) by the MATLAB solver PDEPE and demonstrate the numerical solution profiles. We begin by verifying that system (2.4) can exhibit the bi-stability phenomenon, that is, both toxicant-only steady state $(0, \bar{w})$ and coexistence steady state (u^*, w^*) are locally asymptotically stable. To this end, we choose model parameters within the grey region in Figure 5.1(a) (i.e., $k > k_1$ and $h_1 < h < h_2$). The corresponding numerical simulations are shown in Figure 5.2, where we see that the solution will asymptotically converge to toxicant-only steady state $(0, \bar{w})$ if the initial value is a small perturbation of $(0, \bar{w})$ (see the upper row of Figure 5.2). If the initial value is a small perturbation of coexistence steady state (u^*, w^*), then the solution will asymptotically converge to (u^*, w^*) (see the top row of Figure 5.2). This indicates that in this narrow parameter regimes, the dynamics between the population and the toxicant is very sensitive to the perturbations from the environment and the bi-stability phenomenon may occur.

We next numerically explore whether spatially inhomogeneous patterns can be generated from the model (2.4). As mentioned above, there is no pattern formation bifurcating from the toxicant-only steady state $(0, \bar{w})$. Therefore, we shall examine

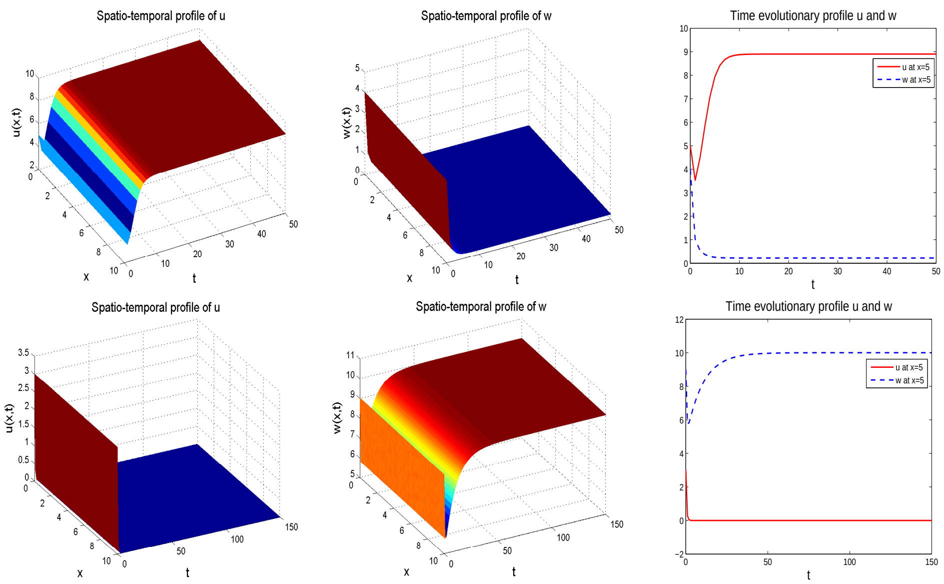

FIG. 5.2. *Numerical simulation for the bistability of the system* (2.4) *with* $r = 1, a = 0.1, m = 0.5, b = 0.5, g = 0.1, d_1 = 0.1, d_2 = 0.1, h = 1, \chi = 0.2,$ *where* $h_1 = 0.2, h_2 = 2.6010, k = 10, k_1 = 0.2, u^* = 8.9012, w^* = 0.2198, \chi_b = 0.9422$. *The initial values for the simulations in the first panel (row) and second panel (row) are chosen as small random perturbations of* (5, 4) *and* (3, 9) *with* 1% *deviation, respectively.*

whether patterns may develop from the coexistence steady state (u^*, w^*) in the instability parameter regimes shown in Theorem 5.1, which entails that (u^*, w^*) becomes unstable if $h < h_1$ or $k > k_1$ and $h_1 \le h < h_2$ provided that $\chi > \chi_b$ as illustrated by the yellow and purple regions in Figure 5.1(b) (color available online). But we do not expect patterns in the purple region since $(0, \overline{w})$ is stable therein. Hence we shall choose model parameters satisfying $h < h_1, \chi > \chi_b$ for numerical simulations with two different cases $k < k_1$ and $k > k_1$. The numerical simulations for the case $k < k_1$ are shown in Figure 5.3, where we do observe the stable spatially inhomogeneous solutions arising from the initial value, which is a small random perturbation of (u^*, w^*). Moreover, we also observe spatial segregation of the population and the toxicant—more (fewer) individuals eventually inhabit locations with low (high) toxicant concentrations (see the right column of Figure 5.3). In this case, the population is abundant, and the toxicant remains at a low level. Next we turn to look at another case $k > k_1$ and plot the numerical solutions of model (2.4) in Figure 5.4. Interestingly we find that apparent spatial segregation between the population and the toxicant will occur, that is, almost all individuals concentrate around the habitat boundary where the toxicant level is the lowest. This gives a more remarkable spatial segregation than that shown in Figure 5.3.

The global stability results in Theorem 2.2 and local stability/instability results in Theorem 5.1 alongside the numerical simulations illustrated above indicate that as long as the toxicant input rate h is suitably small (like $h < h_1$), the population and toxicant may coexist homogeneously in space if toxicant-taxis is weak (i.e., χ is small) or inhomogeneously in space if toxicant-taxis is strong (i.e., χ is large).

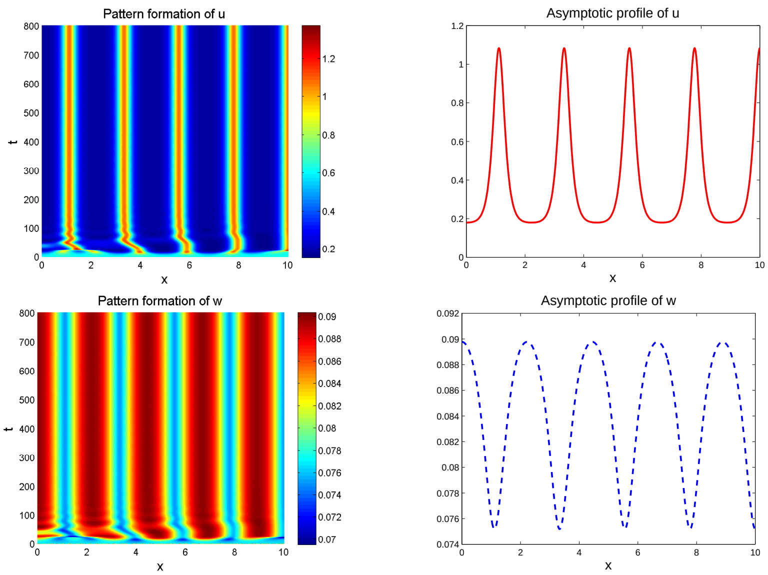

Fig. 5.3. *Numerical simulation for the pattern formation and segregation of the system* (2.4) *with* $r = 1, a = 1, m = 5, b = 0.5, g = 1, d_1 = 0.1, d_2 = 0.1, h = 0.1, \chi = 20$*, where* $h_1 = 0.2, h_2 = 0.2250, k = 1, k_1 = 2, u^* = 0.6180, w^* = 0.0764, \chi_b = 15.2056$*. The initial value* (u_0, w_0) *is a small random perturbation (1% derivation) of the positive steady states* (u^*, w^*)*.*

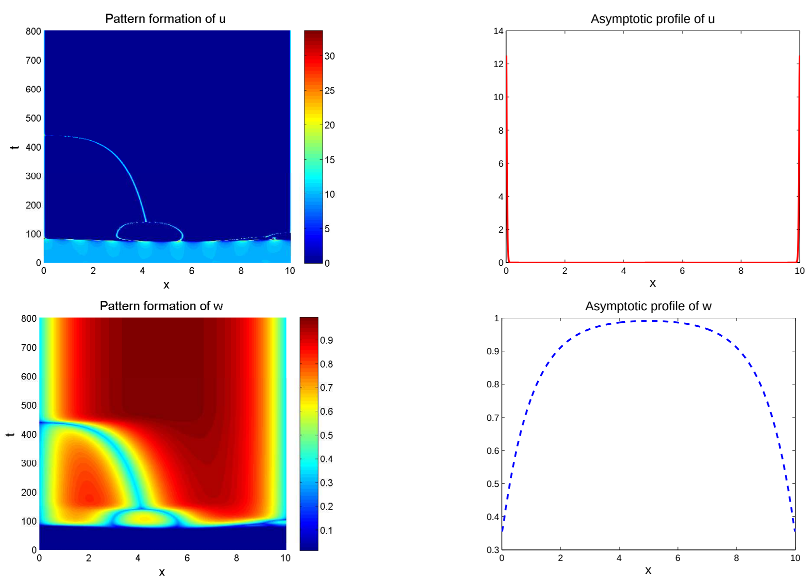

Fig. 5.4. *Numerical simulation for the pattern formation and segregation of the system* (2.4) *with* $r = 1, a = 0.1, m = 0.5, b = 0.5, g = 0.1, d_1 = 0.1, d_2 = 0.1, h = 0.1, \chi = 11$*, where* $h_1 = 0.2, h_2 = 2.6010, k = 10, k_1 = 0.2, u^* = 9.9010, w^* = 0.0198, \chi_b = 10.7029$*. The initial value* (u_0, w_0) *is a small random perturbation (1% derivation) of the positive steady states* (u^*, w^*)*.*

6. Discussion.

Toxicants in polluted water bodies have diverse harmful effects on aquatic species' health. When designing environmental policies to limit the damage caused by water pollution, it is paramount to assess and predict the risk that toxicants pose to aquatic species. However, rigorously testing the effects of toxicants on entire groups of organisms without severely damaging their whole ecosystems is simply not feasible. Mathematical modeling can provide a flexible way to assess toxicants' impact on populations without endangering the environment. Traditional ordinary differential equation models that describe the impact of toxicants on population dynamics do not consider the influences of spatial dispersal of populations and toxicants on population persistence. Taking into account random movements of individuals and toxicants, as well as individuals actively escaping from locations with high toxicant concentrations to locations with low toxicant concentrations, we propose and study a diffusive population-toxicant model with toxicant-taxis. The model can be utilized to understand how the interplay between several factors (toxicant input and degradation, population and toxicant dispersal mechanisms, population growth, and mortality) affects the population dynamics in an aquatic contaminated environment.

We studied the model by analyzing the existence and stability of the toxicant-only steady state $(0,\overline{w})$ at which the population goes extinct as well as the coexistence steady states (u_*,w_*) and (u^*,w^*) at which the population persists. Since the coexistence equilibrium (u_*,w_*) is unstable, we concentrated on the stability analysis of the other two equilibria. We obtained some sufficient conditions under which $(0,\overline{w})$ and (u^*,w^*) are globally asymptotically stable (see Theorem 2.2). As expected, the population can persist only if the toxicant input rate h is small (i.e., $h<h_1$), that is, we are supposed to take measures to limit the toxicant input at low levels to reduce the detrimental effects of toxicants on populations.

To examine whether there exist spatially inhomogeneous steady state solutions driven by spatial dispersal, we further investigate the possibility that the coexistence equilibrium (u^*,w^*) becomes unstable, i.e., the emergence of spatially inhomogeneous patterns. Our findings reveal that random diffusion (i.e., diffusion coefficients) does not lead to instability of coexistence equilibrium, but sufficiently large toxicant-taxis does (see Theorem 5.1). In other words, active flee behavior of individuals away from areas with high toxicant concentrations will generate spatially inhomogeneous distributions of the population and the toxicant in the habitat. This is verified by our numerical simulations (see Figures 5.3 and 5.4).

There are still several problems we are unable to address. First, in Theorem 2.2(i), the global stability of the toxicant-only steady states $(0,\overline{w})$ was proved only in the parameter regime $h>h_3$ or (2.10) but remains open outside these regimes. From the stability results summarized in Table 2.2 and the instability results in Theorem 5.1 (see also Figure 5.1), we conjecture that $(0,\overline{w})$ will be globally asymptotically stable in the regions not shaded in Figure 2.1 and have to leave it open for future study. In Figures 5.3 and 5.4, we have numerically illustrated that spatially inhomogeneous stationary solutions segregated in space exist for the model (2.4). However, how to prove the existence of nonconstant stationary solutions (2.4) with segregation structures remains an interesting open problem for future efforts.

The current work could be generalized in various biologically significant ways: (1) The toxicant input rate is assumed to be spatially heterogeneous in model (2.4). However, toxicants may be released into water bodies at specific times in real-world contexts. Including temporally heterogeneous input rates of the toxicant would result in a more realistic model. (2) A large number of species inhabit an environment with a unidirectional flow, such as rivers and streams. Recently, Zhou and Huang [41] proposed a spatiotemporal model for the effects of toxicants on populations in a polluted river, but their model does not take toxicant-taxis into account. By including advection terms in model (2.4), one can obtain a reaction-diffusion-advection model with toxicant-taxis. (3) Different species that live in a contaminated environment may exhibit considerable differences in their susceptibility to toxicants and the behavioral changes induced by toxicants. Considering two species that compete for the same resources in a polluted habitat [33], one can extend model (2.4) to a competition model and investigate how the toxicant and population dispersal strategies affect the competition outcomes. (4) It is also worthwhile to extend our single-species model (2.4) to a diffusive predator-prey system with toxicant-taxis and investigate how disparities in toxicant vulnerability between the predator and the prey [22], as well as toxicant-induced behavioral changes, affect species persistence, coexistence, and population levels. We anticipate that extending the current model in these ways will yield some interesting mathematical and ecological problems.

Appendix A. Stability analysis of the equilibria of the ODE system (2.6). To determine the local stability of an equilibrium (u_s, w_s), we use the following Jacobian matrix for system (2.6), as long as real parts of eigenvalues of the Jacobian, evaluated at the equilibria, are nonzero:

$$J(u_s, w_s) = \begin{bmatrix} r - 2au_s - mw_s & -mu_s \\ -bw_s & -bu_s - g \end{bmatrix}.$$

The Jacobian matrix evaluated at the toxicant-only equilibrium $(0, \bar{w})$ is

$$J(0, \bar{w}) = \begin{bmatrix} r - m\bar{w} & 0 \\ -b\bar{w} & -g \end{bmatrix},$$

and the eigenvalues are

$$\lambda_1 = r - m\bar{w} = r - mh/g, \quad \lambda_2 = -g.$$

Clearly $\lambda_2 < 0$ due to $g > 0$. When $h > gr/m = h_1$, λ_1 is negative and consequently the equilibrium $(0, \bar{w})$ is a stable node. When $h < h_1$, $\lambda_1 > 0$ and hence $(0, \bar{w})$ is a saddle (hence unstable). If $h = h_1$, then $\lambda_1 = 0$ and so $(0, \bar{w})$ is marginally stable. In particular, if $k = k_1$, then $h_2 = h_1$ and hence $(0, \bar{w})$ is marginally stable in the case $k = k_1$ and $h = h_2$.

For the coexistence equilibrium (u^*, w^*) which only conditionally exists (see (2.9)), one can find that

$$\mathrm{Trace}(J(u^*, w^*)) = r - 2au^* - mw^* - bu^* - g = -au^* - bu^* - g < 0,$$

$$\mathrm{Det}(J(u^*, w^*)) = (r - 2au^* - mw^*)(-bu^* - g) - mbu^*w^* = ab(u^*)^2 - mh + gr.$$

Note that (u^*, w^*) does not exist if $k \le k_1$ and $h \ge h_1$. When $k \le k_1$ and $h < h_1$, one can verify that $\mathrm{Det}(J(u^*, w^*)) > 0$, so (u^*, w^*) is a stable node. When $k > k_1$ and $h < h_2$, one can show that $h < \frac{(ag+br)^2 + (br-ag)\sqrt{\Delta}}{4abm}$, which is equivalent to $ab(u^*)^2 - mh + gr > 0$ (i.e., $\mathrm{Det}(J(u^*, w^*)) > 0$), so the equilibrium (u^*, w^*) is also a stable node.

For the coexistence (u_*, w_*), which exists only if $k > k_1$ and $h_1 < h \le h_2$, we have

$$\mathrm{Trace}(J(u_*, w_*)) = r - 2au_* - mw_* - bu_* - g = -au_* - bu_* - g < 0,$$

but

$$\mathrm{Det}(J(u_*, w_*)) > 0 \Leftrightarrow ab(u_*)^2 - mh + gr > 0 \Leftrightarrow h < h_1.$$

It can be further checked that if $h_1 < h < h_2$, then $\mathrm{Det}(J(u_*, w_*)) < 0$ and (u_*, w_*) is a saddle (hence unstable).

As $k > k_2$ and $h = h_2$, $(u_*, w_*) = (u^*, w^*)$ and $\mathrm{Det}(J(u^*, w^*)) = 0$ which indicates that (u^*, w^*) is marginally stable.

Finally, we show that system (2.6) has no closed orbits. Indeed, choosing $B(u, w) := 1/u$, we have

$$\frac{\partial(BF)}{\partial u} + \frac{\partial(BG)}{\partial w} = -a - b - \frac{g}{u} < 0$$

for $u > 0$ and $w > 0$. By the Bendixson–Dulac criteria [9], there is no closed orbit lying entirely in the first quadrant of the uw-plane. Therefore, by the Poincaré–Bendixson theorem, we get the global stability of $(0, \overline{w})$ as claimed in Table 2.2.

Acknowledgment. The authors are grateful to the anonymous referees for many insightful comments that helped improve the exposition of the paper.

REFERENCES

[1] N. D. Alikakos, *L^p bounds of solutions of reaction-diffusion equations*, Comm. Partial Differential Equations, 4 (1979), pp. 827–868.

[2] H. Amann, *Dynamic theory of quasilinear parabolic systems*, Math. Z., 202 (1989), pp. 219–250.

[3] H. Amann, *Dynamic theory of quasilinear parabolic equations,* II*: Reaction-diffusion systems*, Differential Integral Equations, 3 (1990), pp. 219–250.

[4] H. Amann, *Nonhomogeneous linear and quasilinear elliptic and parabolic boundary value problems, in: Function Spaces*, Differential Operators Nonlinear Anal., (1993), pp. 9–126.

[5] G. J. Atchison, M. G. Henry, and M. B. Sandheinrich, *Effects of metals on fish behavior: A review*, Environ. Biol. Fish., 18 (1987), pp. 11–25.

[6] S. M. Bartell, R. A. Pastorok, H. R. Akçakaya, H. Regan, S. Ferson, and C. Mackay, *Realism and relevance of ecological models used in chemical risk assessment*, Hum. Ecol. Risk Assess., 9 (2003), pp. 907–938.

[7] J. H. S. Blaxter and C. C. T. Hallers-Tjabbes, *The effect of pollutants on sensory systems and behaviour of aquatic animals*, Neth. J. Aquat. Ecol., 26 (1992), pp. 43–58.

[8] J. P. Bourguignon and H. Brezis, *Remarks on the Euler equation*, J. Funct. Anal., 15 (1974), pp. 341–363.

[9] T. A. Burton, *Volterra Integral and Differential Equations*, 2nd ed., Math. Sci. Eng. 202, Elsevier, Amsterdam, 2005.

[10] J. A. Camargo and Á. Alonso, *Ecological and toxicological effects of inorganic nitrogen pollution in aquatic ecosystems: A global assessment*, Environ. Int., 32 (2006), pp. 831–849.

[11] V. Capasso, *Mathematical Structures of Epidemic Systems*, Lecture Notes in Biomath. 97, Springer-Verlag, Berlin, 1993.

[12] W. H. Clements and C. Kotalik, *Effects of major ions on natural benthic communities: An experimental assessment of the US Environmental Protection Agency aquatic life benchmark for conductivity*, Freshw. Sci., 35 (2016), pp. 126–138.

[13] J. W. Fleeger, K. R. Carman, and R. M. Nisbet, *Indirect effects of contaminants in aquatic ecosystems*, Sci. Total Environ., 317 (2003), pp. 207–233.

[14] N. Galic, U. Hommen, J. Baveco, and P. van den Brink, *Potential application of population models in the European ecological risk assessment of chemicals* II*: Review of models and their potential to address environmental protection aims*, Integr. Environ. Assess. Manag., 6 (2010), pp. 338–360.

[15] T. G. Hallam, C. E. Clark, and G. S. Jordan, *Effects of toxicants on populations: A qualitative approach* II*: First order kinetics*, J. Math. Biol., 18 (1983), pp. 25–37.

[16] T. G. Hallam, C. E. Clark, and R. R. Lassiter, *Effects of toxicants on populations: A qualitative approach* I*: Equilibrium environmental exposure*, Ecol. Model., 18 (1983), pp. 291–304.

[17] T. G. Hallam and J. T. De Luna, *Effects of toxicants on populations: A qualitative approach* III*: Environmental and food chain pathways*, J. Theor. Biol., 109 (1984), pp. 411–429.

[18] T. Hanazato, *Pesticide effects on freshwater zooplankton: An ecological perspective*, Environ. Pollut., 112 (2001), pp. 1–10.

[19] D. Henry, *Geometric Theory of Semilinear Parabolic Equations*, Lecture Notes in Math. 840, Springer, Berlin, 2006.
[20] Q. Huang, L. Parshotam, H. Wang, C. Bampfylde, and M. A. Lewis, *A model for the impact of contaminants on fish population dynamics*, J. Theor. Biol., 334 (2013), pp. 71–79.
[21] Q. Huang, G. Seo, and C. Shan, *Bifurcations and global dynamics in a toxin-dependent aquatic population model*, Math. Biosci., 296 (2018), pp. 26–35.
[22] Q. Huang, H. Wang, and M. A. Lewis, *The impact of environmental toxins on predator-prey dynamics*, J. Theor. Biol., 378 (2015), pp. 12–30.
[23] R. Kowalczyk and Z. Szymańska, *On the global existence of solutions to an aggregation model*, J. Math. Anal. Appl., 343 (2008), pp. 379–398.
[24] O. A. Ladyzhenskaya, V. A. Solonnikov, and N. N. Ural'tseva, *Linear and Quasi-linear Equations of Parabolic Type*, Trans. Math. Monogr. 23, AMS, Providence, RI, 1968.
[25] G. Lan, C. Wei, and S. Zhang, *Long time behaviors of single-species population models with psychological effect and impulsive toxicant in polluted environments*, Phys. A, 521 (2019), pp. 828–842.
[26] J. LaSalle, *Some extensions of Lyapunov's second method*, IRE Trans. Circuit Theory, 7 (1960), pp. 520–527.
[27] Z. Ma, G. Cui, and W. Wang, *Persistence and extinction of a population in a polluted environment*, Math. Biosci., 101 (1990), pp. 75–97.
[28] R. Pastorok, R. Akçakaya, H. Regan, S. Ferson, and S. Bartell, *Role of ecological modeling in risk assessment*, Hum. Ecol. Risk Assess., 9 (2003), pp. 939–972.
[29] R. A. Pastorok, S. M. Bartell, S. Ferson, and L. R. Ginzburg, *Ecological Modeling in Risk Assessment: Chemical Effects on Populations, Ecosystems, and Landscapes*, CRC Press, Boca Raton, FL, 2016.
[30] M. M. Porzio and V. Vespri, *Hölder estimates for local solutions of some doubly nonlinear degenerate parabolic equations*, J. Differential Equations, 103 (1993), pp. 146–178.
[31] G. Raugel, *Global attractors in partial differential equations*, Handb. Dyn. Syst., 2 (2002), pp. 887–982.
[32] G. R. Scott and K. A. Sloman, *The effects of environmental pollutants on complex fish behaviour: Integrating behavioural and physiological indicators of toxicity*, Aquat. Toxicol., 68 (2004), pp. 369–392.
[33] C. Shan and Q. Huang, *Direct and indirect effects of toxins on competition dynamics of species in an aquatic environment*, J. Math. Biol., 78 (2019), pp. 739–766.
[34] A. J. Smith and C. P. Tran, *A weight-of-evidence approach to define nutrient criteria protective of aquatic life in large rivers*, J. N. Amer. Benthol. Soc., 29 (2010), pp. 875–891.
[35] R. Temam, *Infinite-Dimensional Dynamical Systems in Mechanics and Physics*, Appl. Math. Sci. 68, Springer-Verlag, New York, 1988.
[36] D. M. Thomas, T. W. Snell, and S. M. Jaffar, *A control problem in a polluted environment*, Math. Biosci., 133 (1996), pp. 139–163.
[37] L. Wu and Z. A. Wang, *Lotka-Volterra diffusion-advection competition system with dynamical resources*, Discrete Contin. Dyn. Syst. Ser. B, 28 (2023), pp. 3322–3348.
[38] B. W. Wolfe and C. G. Lowe, *Movement patterns, habitat use and site fidelity of the white croaker (Genyonemus lineatus) in the Palos Verdes Superfund Site, Los Angeles, California*, Mar. Environ. Res., 109 (2015), pp. 69–80.
[39] S. Yang, F. Xu, F. Wu, S. Wang, and B. Zheng, *Development of PFOS and PFOA criteria for the protection of freshwater aquatic life in China*, Sci. Total Environ., 470 (2014), pp. 677–683.
[40] T. F. Zabel and S. Cole, *The derivation of environmental quality standards for the protection of aquatic life in the UK*, Water Environ. J., 13 (1999), pp. 436–440.
[41] P. Zhou and Q. Huang, *A spatiotemporal model for the effects of toxicants on populations in a polluted river*, SIAM J. Appl. Math., 82 (2022), pp. 95–118, https://doi.org/10.1137/21M1405629.